Title

Contrast-enhanced CT quantification of the hepatic fractional extracellular space: correlation with diffuse liver disease severity.

Journal

American Journal of Roentgenology, 201(6)

ISSN

0361-803X

Authors

Zissen, Maurice H

Wang, Zhen Jane

Yee, Judy

et al.

Publication Date

2013-12-01

DOI

10.2214/ajr.12.10039

Peer reviewed

HHS Public Access

Author manuscript

AJR Am J Roentgenol. Author manuscript; available in PMC 2017 February 20.

Published in final edited form as:

AJR Am J Roentgenol. 2013 December ; 201(6): 1204–1210. doi:10.2214/AJR.12.10039.

Contrast-Enhanced CT Quantification of the Hepatic Fractional Extracellular Space: Correlation With Diffuse Liver Disease Severity

Maurice H. Zissen[1], **Zhen Jane Wang**[1], **Judy Yee**[1], **Rizwan Aslam**[1], **Alexander Monto**[2], and **Benjamin M. Yeh**[1]

[1]Department of Radiology and Biomedical Imaging, University of California, San Francisco, 505 Parnassus Ave, Box 0628, M-372, San Francisco, CA 94143-0628

[2]Department of Internal Medicine, Division of Gastroenterology, San Francisco VA Medical Center, San Francisco, CA

Abstract

OBJECTIVE—The purpose of this study was to determine whether contrast-enhanced CT quantification of the hepatic fractional extracellular space (ECS) correlates with the severity of diffuse liver disease.

MATERIALS AND METHODS—The cases of 70 patients without (46 men, 24 women; mean age, 59.1 years) and 36 patients with (23 men, 13 women; mean age, 63.1 years) cirrhosis who had undergone unenhanced and 10-minute delayed phase contrast-enhanced CT were retrospectively identified. By consensus one experienced radiologist and one trainee measured the CT attenuation of the liver and aorta to estimate the fractional ECS, defined as the ratio of the difference between the attenuation of the liver on 10-minute and unenhanced images to the difference between the attenuation of the aorta on 10-minute and unenhanced images multiplied by 1 minus the hematocrit. Findings were correlated with each patient's Model of End-Stage Liver Disease (MELD) score.

RESULTS—The mean MELD score was higher in patients with than in those without cirrhosis (14.3 ± 7.3 versus 7.20 ± 2.4, $p < 0.0001$). The mean fractional ECS was significantly greater in patients with cirrhosis than in those without cirrhosis (41.0% ± 9.0% versus 23.8% ± 6.3%, $p < 0.0001$). The fractional ECS correlated with the MELD score ($r = 0.572$, $p < 0.0001$) and was predictive of cirrhosis with an area under the receiver operating characteristic curve of 0.953 ($p < 0.0001$). The sensitivity and specificity of an expanded fractional ECS greater than 30% for the prediction of cirrhosis were 92% and 83%. Multivariate linear regression revealed that the fractional ECS is complementary to the MELD score as a predictor of cirrhosis ($p < 0.0001$).

CONCLUSION—Noninvasive contrast-enhanced CT quantification of the fractional ECS correlates with the MELD score, an indicator of the severity of liver disease, and merits further study.

Address correspondence to B. M. Yeh (ben.yeh@ucsf.edu).

Presented at the 2010 annual meeting of the ARRS, San Diego, CA.

Keywords

cirrhosis; CT; delayed enhancement; liver

Diffuse liver disease is a growing public health concern with numerous causes, including viral hepatitis, alcohol, steatohepatitis, and toxins. Although numerous tests are under investigation for the quantification of diffuse liver disease for disease detection and monitoring, each test has limitations. Biopsy is subject to regional sampling and variation in intrareader and interreader interpretation, and serum enzyme panels and metabolic tests do not reliably quantify hepatic parenchymal injury, such as fibrosis [1–6]. Refinements in quantitative CT, MRI, and ultrasound imaging, including elastographic methods, are promising but may require complex modifications of typical imaging protocols and additional institutional expertise and equipment [7–12]. Given the magnitude of diffuse liver disease as a public health concern, alternative simple, noninvasive imaging tests must be explored.

At imaging, liver tissue can be thought of as being composed of three main spaces: the intravascular space, the intracellular space, and the extracellular extravascular space [13–15]. As fibrosis and inflammation occur within the liver, collagen and inflammatory debris expand the extracellular extravascular space, which is within and around the space of Disse located between hepatocytes, vessels, and bile ducts. This finding is one of the essential features used for histopathologic assessment of the severity of diffuse liver disease [16]. The hepatic extracellular extravascular space can be quantified with dynamic contrast-enhanced CT or MRI, but imaging requires rigorous quality control and time-consuming postprocessing, which are difficult for a general radiologist to perform for routine clinical studies [7, 17].

All conventional water-soluble CT contrast agents have a low molecular weight (< 200 Da) and freely exchange between the intravascular and extracellular extravascular spaces. These agents do not accumulate to any substantial degree within the cells of the liver parenchyma and are termed extracellular contrast materials [14, 18]. During the equilibrium phase of liver enhancement, the concentration of contrast material is roughly the same in the fluid of these two compartments, and the sum of the two compartments can be termed the hepatic fractional extracellular space (ECS) (Fig. 1). The fractional ECS can be quantified as the ratio of the enhancement of the liver parenchyma to that of the blood pool (such as blood in the aorta) multiplied by 1 minus hematocrit during the equilibrium phase after parenteral administration of contrast material. Our colleagues [15] described this technique in a preclinical report, but to our knowledge it has not previously been studied clinically for the quantification of diffuse hepatic disease. The purpose of this study is to retrospectively assess whether a simple CT estimate of fractional ECS correlates with the severity of clinical liver disease in a population of patients who have undergone CT and have both unenhanced and equilibrium phase scans available.

Materials and Methods

Patient Selection Criteria

This retrospective case-control study was approved by our institutional review board and did not require informed consent. We performed a computerized search of our radiology information system (IDXrad version 9.7.1, IDX Systems Corporation) for the period January 1, 2005, through August 1, 2009, and identified 425 consecutively registered patients who had undergone CT urography for clinical purposes. This imaging examination includes unenhanced, 90-second delayed (portal venous phase), and 10-minute delayed (equilibrium phase) scans through the abdomen. CT urograms rather than multiphase hepatic CT scans were analyzed because our institutional multiphasic hepatic CT examinations do not routinely include prolonged delayed acquisition during the equilibrium phase of enhancement.

Among the 425 consecutively registered patients, we identified all patients (n = 36; 23 men, 13 women; mean age, 63.1 years; range, 43–88 years) who had a clinical diagnosis of cirrhosis based on review of the clinical medical records and imaging reports. We also randomly included 70 patients without clinical cirrhosis (46 men, 24 women; mean age, 59.1 years; range, 29–89 years). The causes of cirrhosis were hepatitis C (n = 11), alcohol (n = 6), hepatitis B (n = 3), mixed hepatitis and alcohol (n = 4), cryptogenic factors (n = 5), autoimmune disorders (n = 3), toxins (n = 2), and schistosomiasis (n = 1). Of note, our institution is a liver transplant referral center and has a relatively large proportion of patients with liver disease. No patient underwent multiple CT examinations.

CT Protocol

All 106 patients underwent dynamic CT with MDCT scanners (LightSpeed, GE Healthcare). The unenhanced abdominal CT scan parameters were as follows: section thickness, 5 mm; pitch, 1.375; table speed, 13.75 mm/s; maximum tube potential, 140 kVp; and automated tube current modulation to achieve a noise index of 12. The contrast-enhanced CT scans were obtained 90 seconds and 10 minutes after IV administration of 150 mL of iohexol (Omnipaque 350, GE Healthcare) delivered at 3 mL/s with CT scan parameters as follows: section thickness, 1.25 mm; pitch, 1.35; table speed, 13.75 mm/s; maximum tube potential, 120 kVp; automated tube current modulation to achieve a noise index of 12.

Image Review and Clinical Data

At a PACS workstation (Impax, Agfa) two readers (one attending radiologist with 7 years of expertise reading abdominopelvic CT scans and one trainee) jointly reviewed images from all 106 studies by consensus without knowledge of the clinical history. The readers jointly recorded four nonoverlapping CT attenuation measurements of the liver and three attenuation measurements of the aorta at each phase of enhancement using manually drawn circular regions of interest (ROIs) that measured at least 1 cm^2 in diameter (range, 1.0–3.5 cm^2) and were placed with care to avoid blood vessels, areas of artifact, and areas of volume averaging. Two of the ROIs in the liver were placed in the right lobe and two in the left lobe. For unenhanced and 10-minute delayed phase images, reference was made to the 90-second delayed images to best identify regions of liver parenchyma for ROI placement.

The clinical medical records of all patients were subsequently reviewed. For calculation of the Model of End-Stage Liver Disease (MELD) score, the following were recorded: hematocrit; aspartate aminotransferase, alanine aminotransferase, total bilirubin, and alkaline phosphatase, and serum creatinine concentrations; and international normalized ratio. MELD scoring is a system for assessing the severity of chronic liver disease and 3-month mortality among hospitalized patients. A MELD score less than 9 is normal, and a MELD score greater than 40 is predictive of greater than 70% 3-month mortality [19]. The laboratory test results closest to the date of the CT examination were selected for analysis (mean, 41 ± 5 days [standard error of the mean]; range, 0–260 days).

Data and Statistical Analysis

The mean attenuation, in HU, of the liver and aorta at each phase of contrast enhancement was calculated from the previously described ROI measurements. The liver-to-aorta enhancement ratios were calculated at each phase by division of the mean attenuation of the liver by the mean attenuation of the aorta. An estimate of the hepatic fractional ECS volume was calculated as the ratio of the difference between the attenuation of the liver on 10-minute and unenhanced images to the difference between the attenuation of the aorta on 10-minute and unenhanced images multiplied by 1 minus the hematocrit. The relative enhancement of the liver 90 seconds after contrast administration was defined as the liver parenchymal attenuation in HU minus the unenhanced liver attenuation. Continuous variables, including MELD score and CT attenuation measurements, were expressed as mean ± standard error and were tested for significance by Student *t* test.

Unpaired Student *t* tests were used to assess for differences in the means of CT attenuation values between patients with and those without cirrhosis. Pairwise correlation coefficients with the MELD score were obtained for each CT measure. Logistic regression was used to report unit odds ratio with 95% CI, binomial receiver operating characteristic area under the curve (A_z) and sensitivity and specificity after application of optimal cutoff values for fractional ECS and other variables for predicting the presence or absence of cirrhosis. We identified the optimal cutoff by choosing a value of the fractional ECS that maximized the sum of sensitivity and specificity for correct prediction of the presence of cirrhosis. All statistics were calculated with the Stata software package (version 8.0, Stata Corportation). A value of $p < 0.05$ was considered significant.

Results

Descriptive Statistics and Univariate Analysis

The patient demographics and attenuation measurements are summarized in Table 1. Review of the medical records showed that the mean MELD score for all patients was 9.60 ± 0.557 (range, 6–31) and was higher in patients with cirrhosis than in those without (14.3 ± 7.3 versus 7.20 ± 2.4, $p < 0.0001$). For the unenhanced scans, the mean attenuation of the liver was lower in patients with cirrhosis (52.17 ± 7.19 HU) than in those without (56.62 ± 8.96 HU) ($p < 0.05$). On the 10-minute delayed scans, the mean liver-to-aorta ratios were significantly different between patients with cirrhosis (0.987 ± 0.108 HU) and those without

(0.842 ± 0.114 HU) ($p < 0.0001$). Figures 2 and 3 show representative unenhanced, portal venous, and 10-minute delayed phase images of patients with and without cirrhosis.

The distribution of MELD scores is illustrated in Figure 4. Most of the MELD scores in patients without cirrhosis were less than 10 (63/70, 90%), whereas the distribution in patients with cirrhosis was wider: 16 of 36 (44.4%) had MELD scores of 10–20, and seven patients (19.4%) had MELD scores greater than 20.

Figure 5 shows that the mean hepatic fractional ECS volume was statistically significantly greater in patients with cirrhosis than in those without cirrhosis (41.0% ± 9.0% versus 23.8% ± 6.3%, $p < 0.0001$). In addition, a positive correlation was observed between hepatic fractional ECS volume and MELD score ($r = 0.572$, $p < 0.0001$) (Fig. 6). Table 2 outlines the pairwise correlation coefficients between sampled CT measurements and MELD score. For every 10% increase in the calculated hepatic fractional ECS, we observed a 12.2-fold increase in the likelihood that clinical cirrhosis was present (odds ratio, 12.2; 95% CI, 11.3–13.1; $p < 0.0001$).

Receiver Operative Characteristic Analysis

The results of receiver operator curve analysis are shown in Figure 7. They show that hepatic fractional ECS is predictive of the presence of cirrhosis with a diagnostic accuracy A_z of 0.953 (95% CI, 0.918–0.988). The A_z for fractional ECS was significantly greater than the A_z for MELD score in the prediction of cirrhosis (0.815; 95% CI, 0.717–0.912) ($p < 0.05$). The sensitivity and specificity of an expanded hepatic fractional ECS greater than 30% of the hepatic volume for predicting cirrhosis were 92% and 83%.

Discussion

Our results show that a simple quantitative CT estimate of hepatic fractional ECS is predictive of clinical cirrhosis and correlates with the severity of liver disease as predicted with the MELD score. Receiver operating characteristic analysis showed the diagnostic accuracy of fractional ECS for prediction of the presence of clinical cirrhosis was 0.953 (95%), significantly higher than the corresponding diagnostic accuracy of MELD. Although our study was retrospective and performed with a clinical diagnosis of cirrhosis based on review of the medical records rather than histopathologic examination as the primary standard of reference, our promising results show that further prospective study is warranted. The monitoring of diffuse hepatic disease, particularly fibrosis, has been a topic of great interest. Researchers anticipate that accurate and sensitive monitoring of early disease may lead to improvements in the application of therapy to such conditions as hepatitis C, nonalcoholic steatohepatitis, and alcoholic liver disease [17, 19, 20].

Our method of estimating the hepatic fractional ECS volume exploits the well-known high permeability of the hepatic vasculature for conventional extracellular low-molecular-weight contrast material, which may exhibit 20–50% leak out of the intravascular space into the extracellular extravascular space during the first pass of a contrast bolus through the hepatic vascular bed. For our simple estimate of fractional ECS, it is important to acquire images after the concentrations of contrast material in the extracellular extravascular space and the

intravascular space are approximately equal and after the blood pool is close to homogeneous in contrast concentration. Because the human blood circulation time can range from 60 to 90 seconds, a 10-minute delay would allow 6–10 recirculations by the time of imaging. Even though the concentration of intravascular contrast material decreases dramatically within a few minutes after administration, a substantial amount of contrast material remains in the body even after 1 hour because the elimination half-life of conventional contrast material is estimated to be 60 minutes [21]. The dramatic decrease in intravascular contrast material within the first several minutes after administration is due to dispersion and equilibration of contrast material into the approximately 3.5 L of intravascular space and the approximately 10.5 L of extracellular extravascular space. Previous work has shown that little contrast material enters into living cells. Because the blood pool is 100% intravascular space, the relative enhancement of tissue during the equilibrium phase compared with the blood pool corresponds to the relative amount of ECS in that tissue.

Inherent errors in these estimates occur because the relative space taken up by RBCs can vary between the aorta and tissue capillaries and because the extracellular extravascular space contains a variable volume of connective tissue and matrix. Additional error may occur when the extracellular extravascular space is particularly large relative to the quantity and distribution of blood vessels because it will take longer for the concentrations of contrast material in the extracellular extravascular space to increase to that of the intravascular space because contrast medium must diffuse across a larger distance. For this reason, it is important to wait a sufficient time for approximate equilibrium to be reached between the extracellular extravascular space and the intravascular space. A potential limitation is that with long scan delays when there is little remaining contrast material in the body, noise will contribute to measurement errors.

Previous work has shown that scar tissue exhibits high contrast enhancement relative to normal liver parenchyma during the equilibrium phase. For example, delays longer than 10 minutes are useful for highlighting the cicatricial tissue in cholangiocarcinomas and the central scar of focal nodular hyperplasia [12, 22–31]. Furthermore, the delayed enhancement of hepatic septal fibrosis relative to hepatic regenerative nodules in chronic hepatitis is well known [7, 32]. Our results build on this body of previous work and suggest that global liver disease correlates with relative global delayed enhancement, likely because of the known expansion of the ECS by fibrosis and scar in a cirrhotic liver [16]. The current reference standard for the detection and grading of fibrosis is liver biopsy, which is expensive and carries inherent risk of infection, bleeding, and pain, particularly in patients with cirrhosis. Only a small fraction of patients with liver disease ever undergo this invasive test. Furthermore, recent results have suggested that because of sampling error and interobserver variability, there can be up to 30% error in the diagnosis of cirrhosis based on biopsy results [1, 3, 5].

Although CT has traditionally been limited to assessment of the secondary characteristics of cirrhosis, such as liver contour abnormalities and the sequelae of portal hypertension, its use would be ideal in the assessment of cirrhosis because of its speed, ease of acquisition, lack of operator dependence, relative lack of artifact, and importantly, the linear relation between

contrast concentration and CT attenuation. Because of the ubiquity of CT in clinical practice, CT would be an ideal modality for imaging hepatic fibrosis, and it could be an additional tool for acquiring prognostic information during the early stage of cirrhosis. There is the potential that the CT method we describe could be adapted to MRI to minimize exposure of patients to ionizing radiation. The caveat is that quantitative or semiquantitative evaluation of gadolinium concentration may be required. However, both CT and MRI techniques may be limited in patients with advanced liver disease and impaired renal function who cannot tolerate the contrast load or may be at risk of nephrogenic systemic fibrosis.

Hepatic perfusion is considerably decreased in patients with cirrhosis and inversely correlates with the severity of chronic liver disease [8, 11, 12]. Our results are consistent with those of previous studies and show significantly reduced relative liver-to-aorta enhancement at 90 seconds, which may reflect decreased hepatic blood flow and increased portal hypertension. However, to our knowledge, no previous studies have evaluated single-time-point relative liver-to-aorta enhancement during the 10-minute delayed phase of CT enhancement in patients with cirrhosis. Our finding that relative liver-to-aorta enhancement on 10-minute delayed images was significantly elevated in patients with cirrhosis likely reflects contrast equilibration between the vasculature and the extensive interstitial hepatic fibrosis seen in cirrhosis, leading to an extended washout period and contrast trapping. This finding is consistent with those of studies of the optimal time point for delayed enhancement of fibrosis within mass lesions, such as cholangiocarcinoma and adrenal adenomas. The investigators in those studies concluded that after 10 minutes, the mass lesion is maximally hyper-attenuating relative to the surrounding tissues and blood vessels [26, 33, 34].

Our study had several limitations. First, the study was retrospective, and therefore there was a variable time interval between collection of the clinical information and CT acquisition. Second, we did not have a histologic reference standard for correlation with CT because liver biopsy is not routinely performed for this patient population at our institution. Therefore, the MELD score served as a surrogate estimate of disease severity. Because it is affected by clinical variables such as dehydration, infection, and malnutrition, the MELD score is only a rough estimate of the severity of liver disease and may even be normal in some patients with cirrhosis. Nevertheless, our results show the high value of fractional ECS for predicting clinical cirrhosis and liver disease severity. Because estimates of the fractional ECS are simple to obtain, further study is warranted to assess whether this value can improve on the MELD score as a clinical predictor of 3-month mortality among hospitalized patients with chronic liver disease or serve as a screen or surrogate for liver biopsy and elastography. Trials to obtain histologic correlation for measures of fractional ECS are underway at our institution. The findings of the current study serve as an initial description of a novel method that is substantially different from previously described clinical methods of quantifying diffuse liver disease. They also build on previous preclinical results [15] that showed a strong correlation between fractional ECS measures and liver fibrosis in rats.

A third limitation was that the 10-minute delayed phase CT acquisition is not a standard part of routine liver imaging. Nevertheless, similar delayed imaging has become accepted protocol for other visceral evaluations, such as assessment of the urinary collecting system

and adrenal masses. A fourth limitation was that the unenhanced scan was acquired at 140 kVp, and the contrast-enhanced scan was acquired at 120 kVp. This difference might have resulted in slight inaccuracy in the attenuation measurements because certain materials, such as iron, have slightly higher attenuation at 120 kVp than at 140 kVp, and others, such as fat, have lower attenuation. However, this systematic error was likely corrected in part by our use of the ratio of attenuation differences between the liver and aorta. Better results may be obtained by use of the same tube voltage setting for unenhanced and contrast-enhanced imaging. Fifth, we did not evaluate conditions that may affect contrast material equilibrium. For example, contrast material is known to diffuse readily into ascites [14]. Further work is warranted to refine the technique to quantify fractional ECS and determine whether this method is of sufficient value for clinical use.

Notwithstanding the limitations, our results show that a noninvasive method of CT quantification of the hepatic fractional ECS volume may be used to differentiate the presence and absence of clinical cirrhosis and potentially grade the severity of diffuse liver disease.

Acknowledgments

Supported by a grant from GE Healthcare.

References

1. Froehlich F, Lamy O, Fried M, Gonvers JJ. Practice and complications of liver biopsy: results of a nationwide survey in Switzerland. Dig Dis Sci. 1993; 38:1480–1484. [PubMed: 8344104]
2. Grigorescu M. Noninvasive biochemical markers of liver fibrosis. J Gastrointestin Liver Dis. 2006; 15:149–159. [PubMed: 16802010]
3. Maharaj B, Maharaj RJ, Leary WP, et al. Sampling variability and its influence on the diagnostic yield of percutaneous needle biopsy of the liver. Lancet. 1986; 1:523–525. [PubMed: 2869260]
4. Poynard T, McHutchison J, Manns M, Myers RP, Albrecht J. Biochemical surrogate markers of liver fibrosis and activity in a randomized trial of peginterferon alfa-2b and ribavirin. Hepatology. 2003; 38:481–492. [PubMed: 12883493]
5. Regev A, Berho M, Jeffers LJ, et al. Sampling error and intraobserver variation in liver biopsy in patients with chronic HCV infection. Am J Gastroenterol. 2002; 97:2614–2618. [PubMed: 12385448]
6. Sebastiani G, Halfon P, Castera L, et al. SAFE biopsy: a validated method for large-scale staging of liver fibrosis in chronic hepatitis C. Hepatology. 2009; 49:1821–1827. [PubMed: 19291784]
7. Aguirre DA, Behling CA, Alpert E, Hassanein TI, Sirlin CB. Liver fibrosis: noninvasive diagnosis with double contrast material-enhanced MR imaging. Radiology. 2006; 239:425–437. [PubMed: 16641352]
8. Hashimoto K, Murakami T, Dono K, et al. Assessment of the severity of liver disease and fibrotic change: the usefulness of hepatic CT perfusion imaging. Oncol Rep. 2006; 16:677–683. [PubMed: 16969479]
9. Hotta N, Ayada M, Okumura A, et al. Noninvasive assessment of liver disease: measurement of hepatic fibrosis using tissue strain imaging. Clin Imaging. 2007; 31:87–92. [PubMed: 17320774]
10. Stebbing J, Farouk L, Panos G, et al. A meta-analysis of transient elastography for the detection of hepatic fibrosis. J Clin Gastroenterol. 2009; 44:214–219.
11. Van Beers BE, Leconte I, Materne R, Smith AM, Jamart J, Horsmans Y. Hepatic perfusion parameters in chronic liver disease: dynamic CT measurements correlated with disease severity. AJR. 2001; 176:667–673. [PubMed: 11222202]

12. Vignaux O, Legmann P, Coste J, Hoeffel C, Bonnin A. Cirrhotic liver enhancement on dual-phase helical CT: comparison with noncirrhotic livers in 146 patients. AJR. 1999; 173:1193–1197. [PubMed: 10541087]
13. Sahin S, Rowland M. Estimation of aqueous distributional spaces in the dual perfused rat liver. J Physiol. 2000; 528:199–207. [PubMed: 11018118]
14. Benedetti N, Aslam R, Wang ZJ, et al. Delayed enhancement of ascites after i.v. contrast material administration at CT: time course and clinical correlation. AJR. 2009; 193:732–737. [PubMed: 19696286]
15. Varenika V, Fu Y, Maher JJ, et al. Hepatic fibrosis: evaluation with semiquantitative contrast-enhanced CT. Radiology. 2013; 266:151–158. [PubMed: 23169796]
16. Afdhal NH, Nunes D. Evaluation of liver fibrosis: a concise review. Am J Gastroenterol. 2004; 99:1160–1174. [PubMed: 15180741]
17. Bonekamp S, Kamel I, Solga S, Clark J. Can imaging modalities diagnose and stage hepatic fibrosis and cirrhosis accurately? J Hepatol. 2009; 50:17–35. [PubMed: 19022517]
18. Mitchell, DG. MRI principles. Philadelphia, PA: WB Saunders; 1999.
19. Brancatelli G, Federle MP, Ambrosini R, et al. Cirrhosis: CT and MR imaging evaluation. Eur J Radiol. 2007; 61:57–69. [PubMed: 17145154]
20. Thabut D, Simon M, Myers RP, et al. Noninvasive prediction of fibrosis in patients with chronic hepatitis C. Hepatology. 2003; 37:1220–1221. [PubMed: 12717403]
21. Bettmann MA. Frequently asked questions: iodinated contrast agents. RadioGraphics. 2004; 24(suppl 1):S3–S10. [PubMed: 15486247]
22. Asayama Y, Yoshimitsu K, Irie H, et al. Delayedphase dynamic CT enhancement as a prognostic factor for mass-forming intrahepatic cholangiocarcinoma. Radiology. 2006; 238:150–155. [PubMed: 16304089]
23. Brancatelli G, Baron RL, Federle MP, Sparacia G, Pealer K. Focal confluent fibrosis in cirrhotic liver: natural history studied with serial CT. AJR. 2009; 192:1341–1347. [PubMed: 19380559]
24. Iannaccone R, Laghi A, Catalano C, et al. Hepatocellular carcinoma: role of unenhanced and delayed phase multi-detector row helical CT in patients with cirrhosis. Radiology. 2005; 234:460–467. [PubMed: 15671002]
25. Itai Y, Ohtomo K, Kokubo T, et al. CT of hepatic masses: significance of prolonged and delayed enhancement. AJR. 1986; 146:729–733. [PubMed: 3006461]
26. Keogan MT, Seabourn JT, Paulson EK, McDermott VG, Delong DM, Nelson RC. Contrast-enhanced CT of intrahepatic and hilar cholangiocarcinoma: delay time for optimal imaging. AJR. 1997; 169:1493–1499. [PubMed: 9393152]
27. Koh TS, Thng CH, Hartono S, et al. Dynamic contrast-enhanced CT imaging of hepatocellular carcinoma in cirrhosis: feasibility of a prolonged dual-phase imaging protocol with tracer kinetics modeling. Eur Radiol. 2009; 19:1184–1196. [PubMed: 19137312]
28. Lacomis JM, Baron RL, Oliver JH 3rd, Nalesnik MA, Federle MP. Cholangiocarcinoma: delayed CT contrast enhancement patterns. Radiology. 1997; 203:98–104. [PubMed: 9122423]
29. Ohtomo K, Baron RL, Dodd GD 3rd, et al. Confluent hepatic fibrosis in advanced cirrhosis: appearance at CT. Radiology. 1993; 188:31–35. [PubMed: 8511316]
30. Yoshikawa J, Matsui O, Kadoya M, Gabata T, Arai K, Takashima T. Delayed enhancement of fibrotic areas in hepatic masses: CT-pathologic correlation. J Comput Assist Tomogr. 1992; 16:206–211. [PubMed: 1312098]
31. Gabata T, Matsui O, Kadoya M, et al. Delayed MR imaging of the liver: correlation of delayed enhancement of hepatic tumors and pathologic appearance. Abdom Imaging. 1998; 23:309–313. [PubMed: 9569304]
32. Semelka RC, Chung JJ, Hussain SM, Marcos HB, Woosley JT. Chronic hepatitis: correlation of early patchy and late linear enhancement patterns on gadolinium-enhanced MR images with histopathology initial experience. J Magn Reson Imaging. 2001; 13:385–391. [PubMed: 11241811]
33. Blake MA, Kalra MK, Sweeney AT, et al. Distinguishing benign from malignant adrenal masses: multi-detector row CT protocol with 10-minute delay. Radiology. 2006; 238:578–585. [PubMed: 16371582]

34. Kamiyama T, Fukukura Y, Yoneyama T, Takumi K, Nakajo M. Distinguishing adrenal adenomas from nonadenomas: combined use of diagnostic parameters of unenhanced and short 5-minute dynamic enhanced CT protocol. Radiology. 2009; 250:474–481. [PubMed: 19037020]

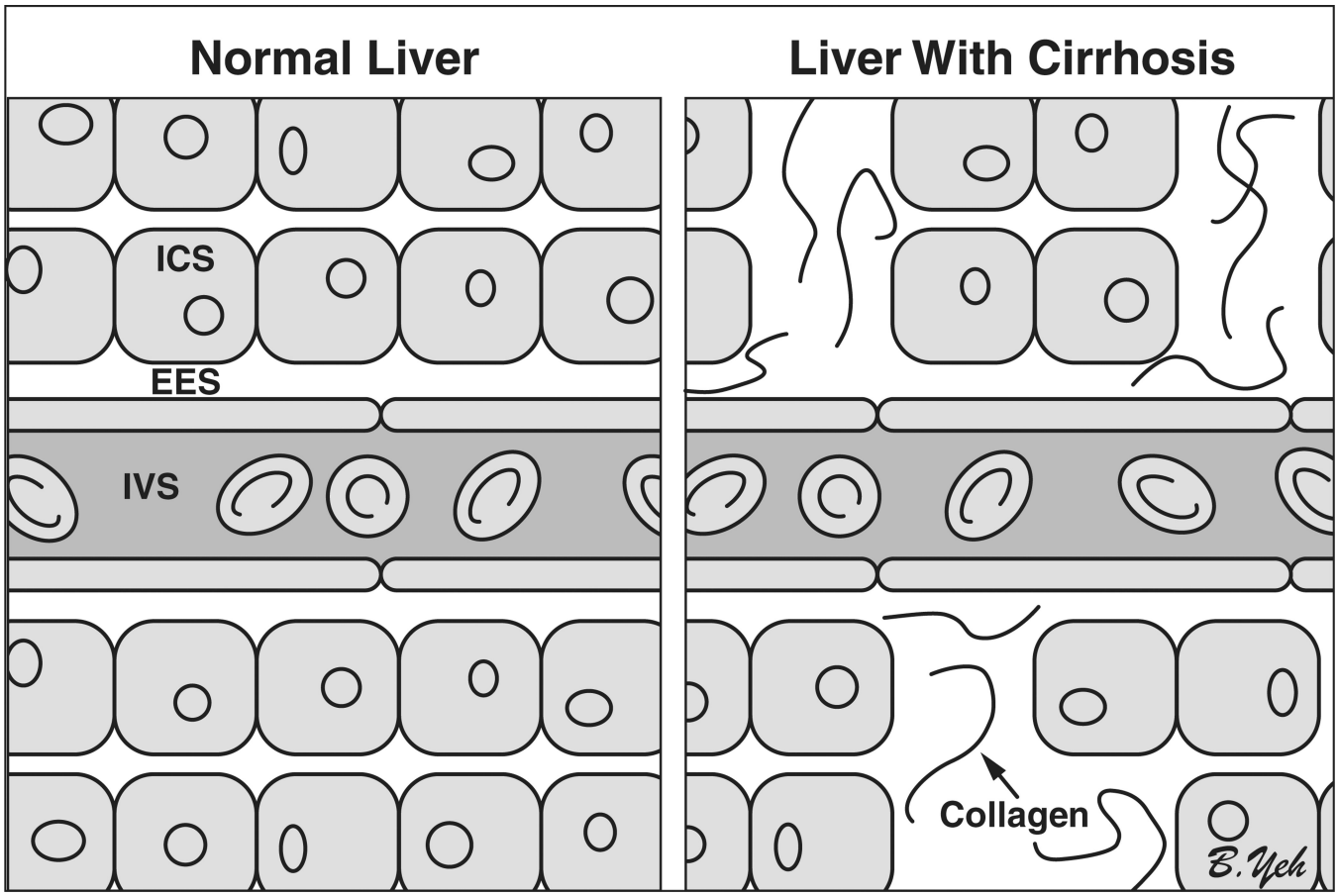

Fig. 1.

Diagram shows liver spaces. Microscopic tissue spaces can be categorized simply as intracellular space (ICS), extracellular extravascular space (EES), and intravascular space (IVS). Extracellular space (ECS) is sum of EES and IVS. Commercially available CT contrast material is known as extracellular contrast material because it equilibrates rapidly between EES and IVS but does not readily enter into living cells. This property allows simple quantification of ECS during equilibrium phase at CT. EES of normal liver is small, but in liver affected by cirrhosis, EES is markedly expanded owing to collagen deposition.

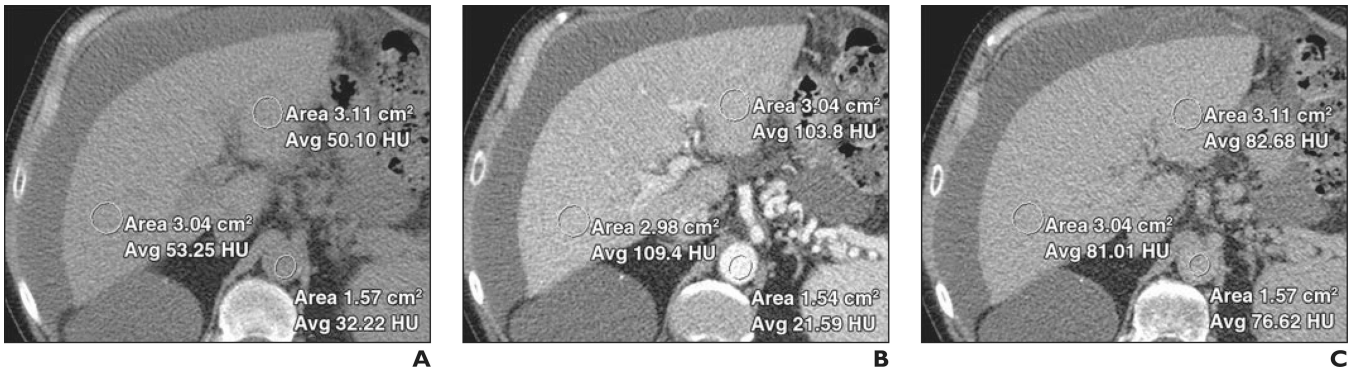

Fig. 2. 80-year-old man with cirrhosis

A–C, Axial unenhanced (**A**), 90-second delayed (**B**), and 10-minute delayed (**C**) CT scans show regions of interest placed on liver parenchyma and aorta. Fractional extracellular space is 39.5%, and Model of End-Stage Liver Disease score is 21.

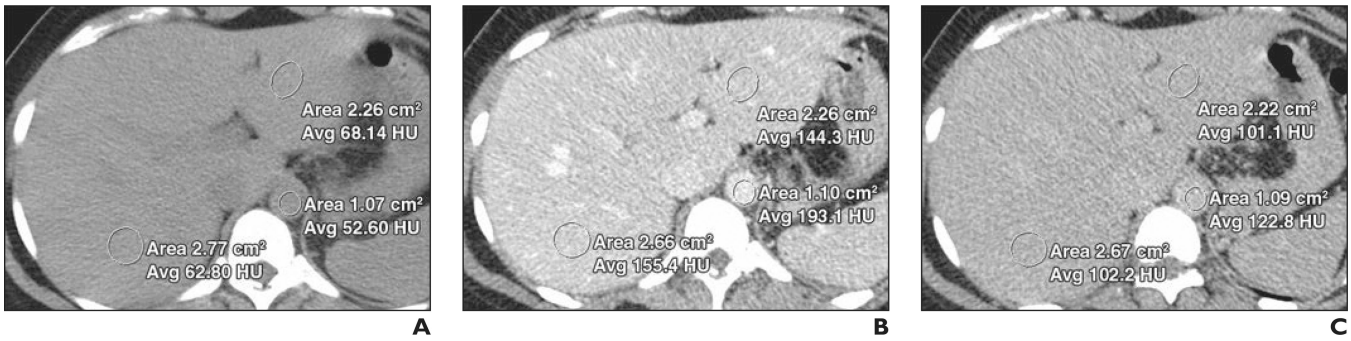

Fig. 3. 35-year-old woman without cirrhosis

A–C, Axial unenhanced (**A**), 90-second delayed (**B**), and 10-minute delayed (**C**) CT scans show regions of interest placed on liver parenchyma and aorta. Fractional extracellular space is 26.4%, and Model of End-Stage Liver Disease score is 7.

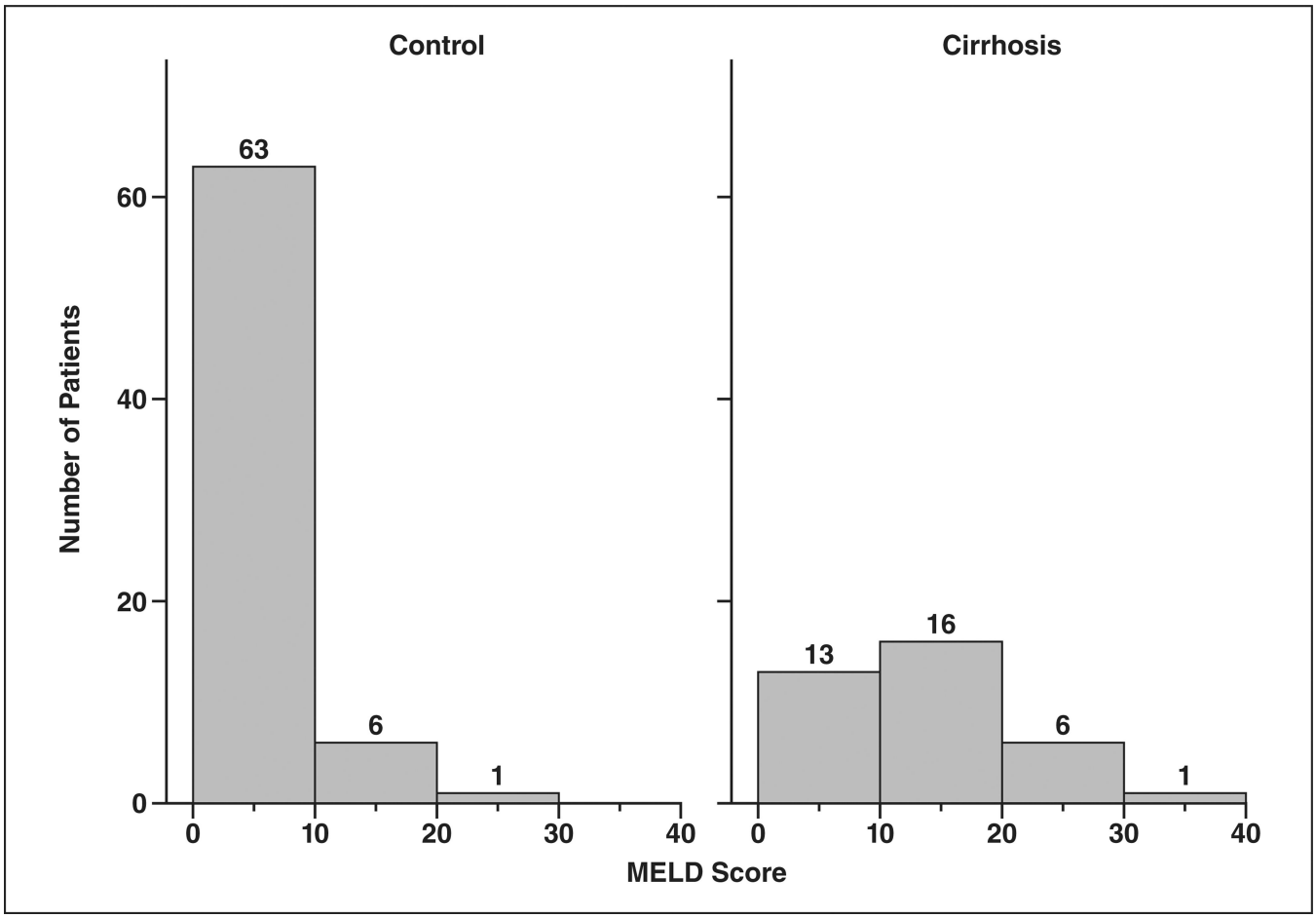

Fig. 4.

Histogram shows distribution of Model of End-Stage Liver Disease (MELD) scores in patients without (*left*) and with (*right*) cirrhosis.

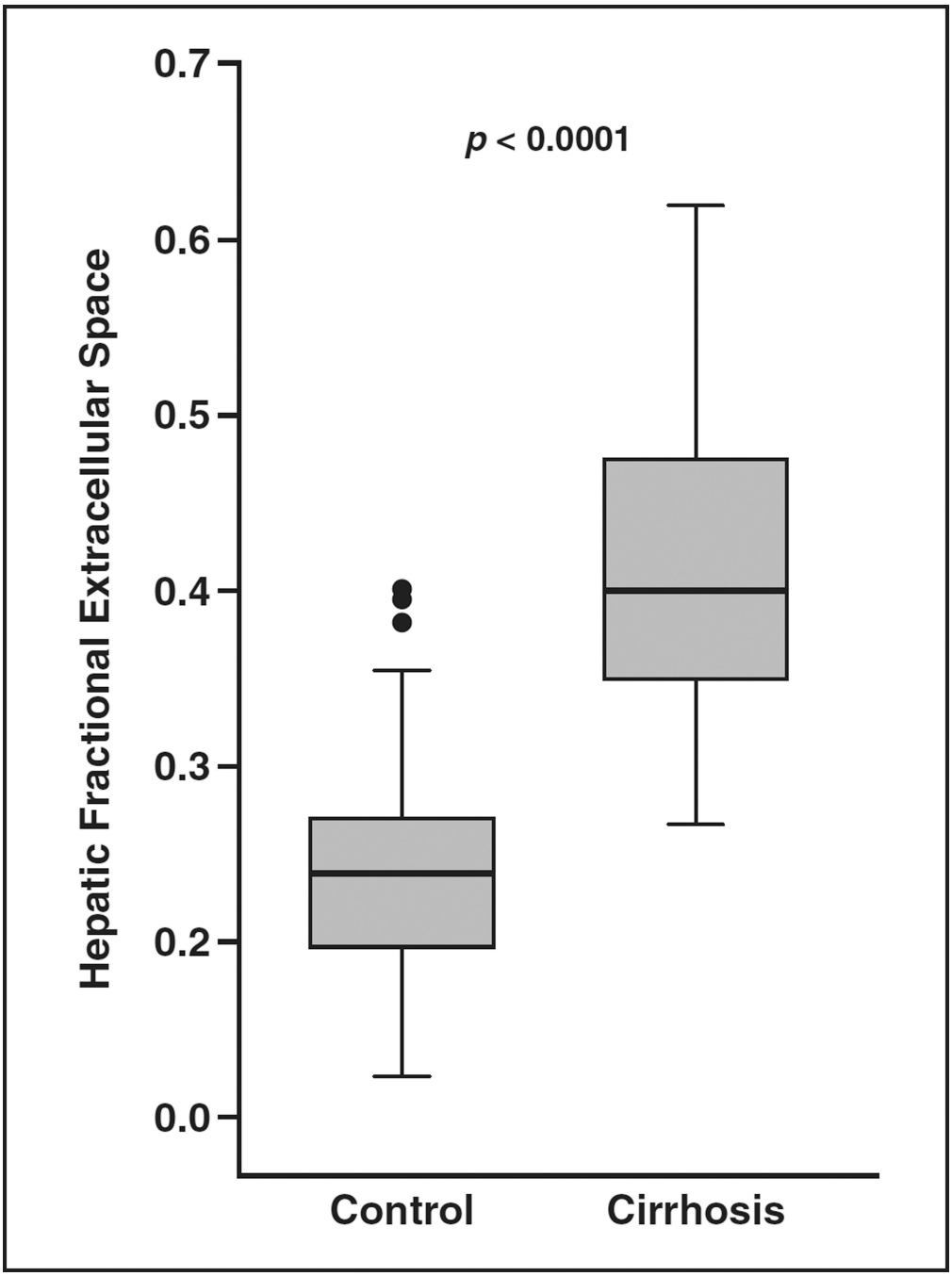

Fig. 5.
Box plot shows difference in CT estimate of hepatic fractional extracellular space between patients without and those with cirrhosis.

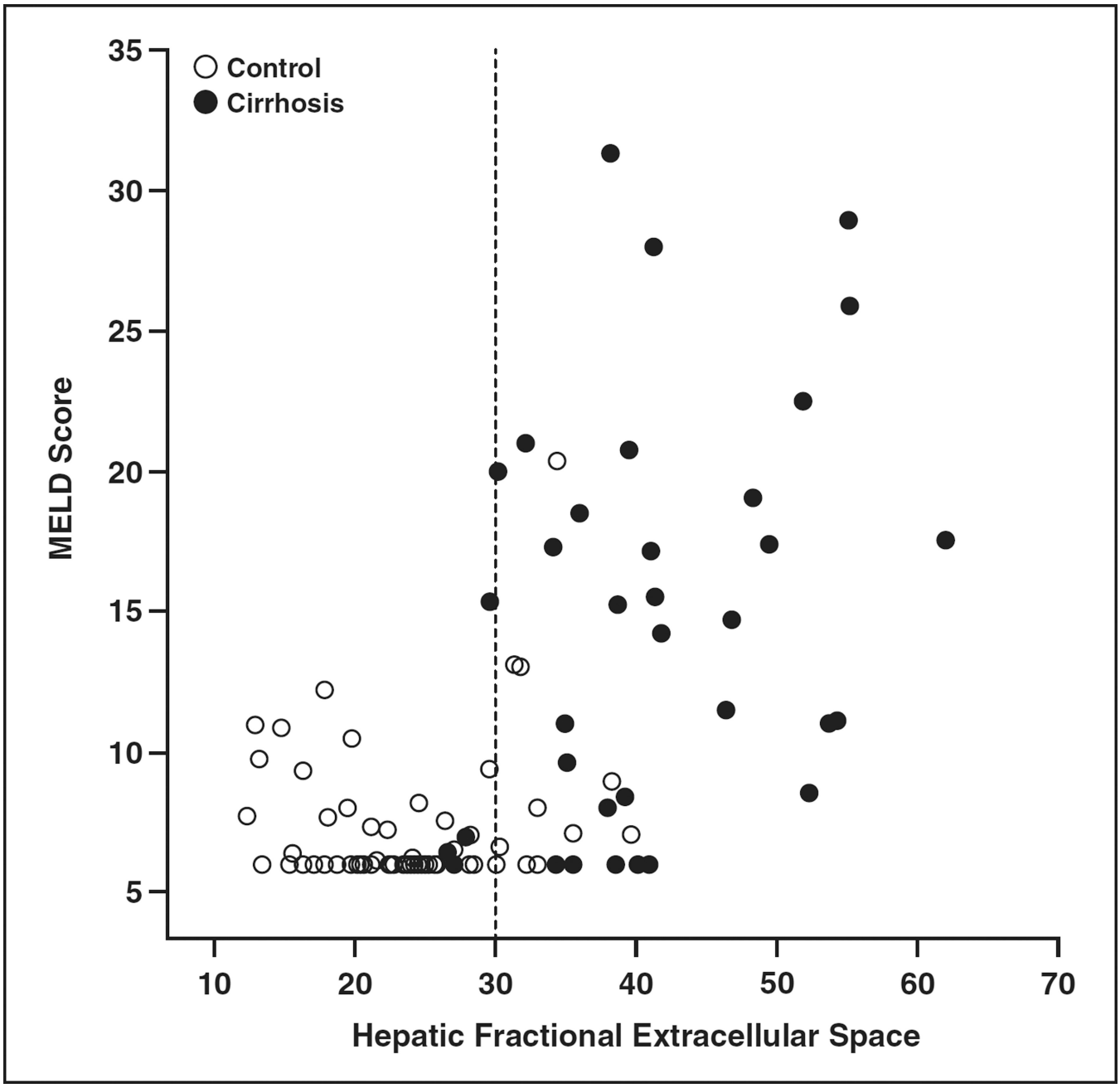

Fig. 6.

Scatterplot shows fractional hepatic extracellular space versus Model of End-Stage Liver Disease (MELD) score in patients without (control) and those with cirrhosis.

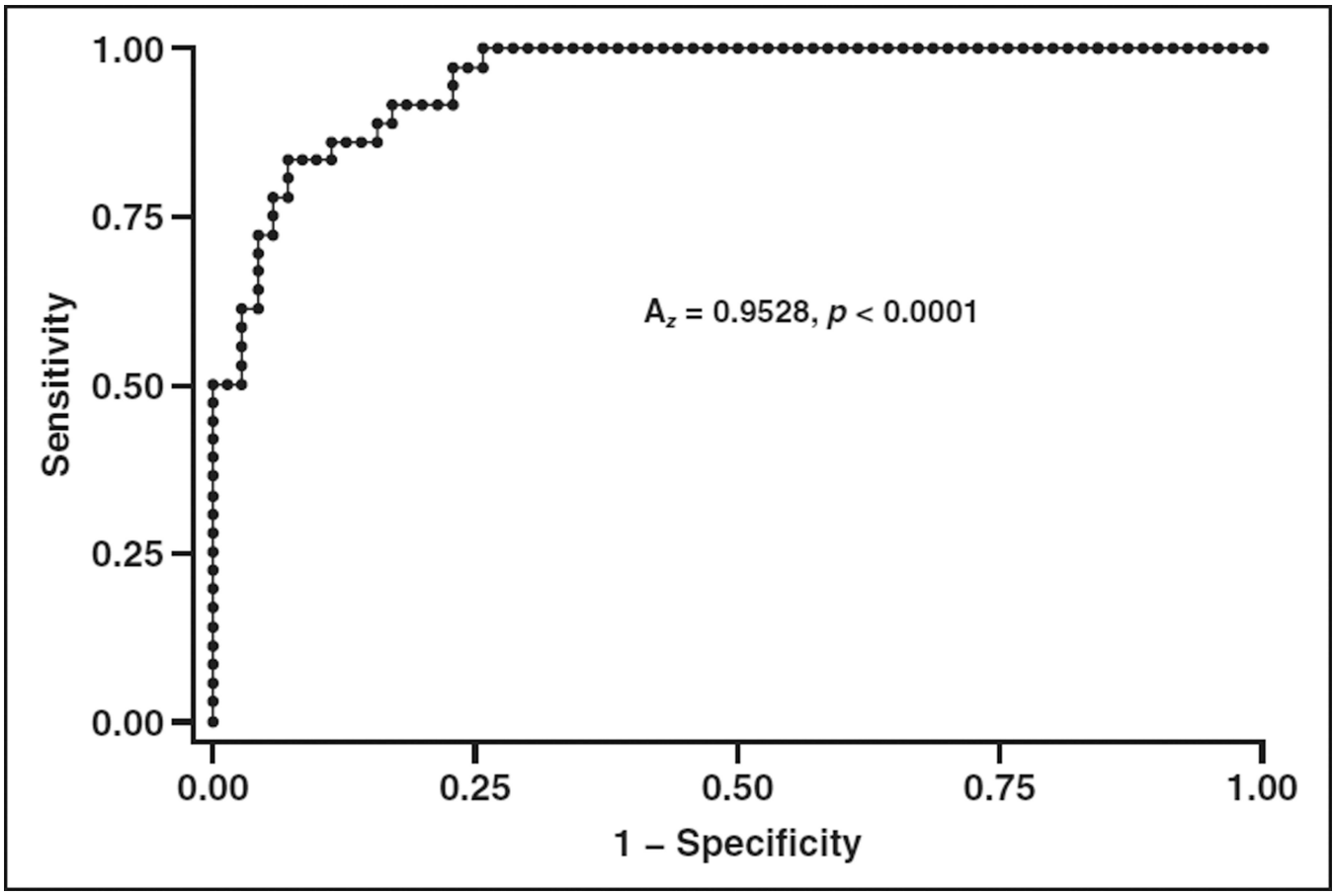

Fig. 7.

Receiver operating characteristic curve for fractional hepatic extracellular space (ECS) in prediction of cirrhosis. Area under the curve (A_z) for fractional ECS in prediction of cirrhosis is 0.953 (95% CI, 0.918–0.988) and is significantly greater than A_z for Model of End-Stage Liver Disease score in prediction of cirrhosis (not shown) (0.815; 95% CI, 0.717–0.912) ($p < 0.05$).

TABLE 1

Demographic Data, Clinical Data, and Imaging Findings

Characteristic	Patients With Cirrhosis	Patients Without Cirrhosis	*p*
Demographics			
Total no. of patients	36	70	
Age (y)			0.201
Mean ± SD	63 ± 12.35	59 ± 16.06	
Range	43–88	29–89	
Sex			0.658
Men	23 (63.9)	46 (65.7)	
Women	13 (36.1)	24 (34.3)	
Clinical data[a]			
Hematocrit (%)	33.8 ± 6.5	40.3 ± 5.7	< 0.0001
Serum creatinine concentration (mg/dL)	1.14 ± 0.54	0.93 ± 0.28	< 0.05
Total bilirubin concentration (mg/dL)	3.84 ± 5.84	0.87 ± 0.39	< 0.0001
International normalized ratio	1.54 ± 0.61	1.12 ± 0.57	< 0.0001
Model of End-Stage Liver Disease score			< 0.0001
Mean ± SD	14.3 ± 7.3	7.2 ± 2.4	
Range	6–31	6–20	
CT liver-to-aorta enhancement ratio (HU)[a]			
Unenhanced scan	1.59 ± 0.38	1.71 ± 0.52	0.194
90-s delayed	0.590 ± 0.159	0.661 ± 0.147	< 0.05
10-min delayed	0.987 ± 0.108	0.842 ± 0.114	< 0.0001
Hepatic fractional extracellular space (%)[b]	41.0 ± 9.0	23.8 ± 6.3	< 0.0001

Note—Values in parentheses are percentages.

[a] Values are mean ± SD.

[b] [(10-minute liver – unenhanced liver) / (10-minute aorta – unenhanced aorta) × (1 – hematocrit)].

TABLE 2

Pairwise Correlation Between CT Measurements and Model of End-Stage Liver Disease (MELD) Score

CT Measurement	*R*	*p*
Liver-to-aorta enhancement ratio		
Unenhanced scans	0.055	0.575
90-s delayed scans	0.021	0.828
10-min delayed scans	0.489[a]	< 0.0001
Hepatic fractional extracellular space	0.572[a]	< 0.0001

[a]Significant at 0.01 level (two-tailed).